Available online at www.sciencedirect.com

jmr&t Journal of Materials Research and Technology

www.jmrt.com.br

Original Article

Ferrite content meter analysis for delta ferrite evaluation in superduplex stainless steel☆

Cesar G. Camerini[a,*], Vitor Manoel A. Silva[a], Iane A. Soares[a], Rafael Wagner F. Santos[b], Julio Endress Ramos[b], João Marcio C. Santos[b], Gabriela Ribeiro Pereira[a]

[a] Federal University of Rio de Janeiro, Laboratory of Non Destructive Testing, Corrosion and Welding - COPPE/UFRJ, Rio de Janeiro, RJ, Brazil

[b] CENPES – PETROBRAS Research Centre, Rio de Janeiro, RJ, Brazil

ARTICLE INFO

Article history:
Received 20 November 2017
Accepted 10 June 2018
Available online 1 August 2018

Keywords:
Superduplex stainless steel
Ferrite content meter
Calibration procedures
X-ray diffraction

ABSTRACT

Superduplex stainless steel is a widely used material in many industrial areas, due to its significant properties in terms of mechanical and corrosion resistance. In order to guarantee the quality of these steels, the ferrite evaluation is an important analysis since many properties depend on the control of the ferrite content. During equipment manufacturing or field inspections, the most conventional way to evaluate the ferrite content is through ferritoscope measurements, due to its portability and easy interpretation. However, it has been observed that the calibration pattern used for ferritoscope calibration can lead to inaccurate ferrite quantification in superduplex inspection. In order to analyze this influence, different characterization techniques were performed in superduplex samples, such as optical microscopy, X-ray diffraction, and vibrating sample magnetometer, to compare with the measurements obtained by a ferritoscope. It was concluded that for high ferrite values, with the calibration made from the calibration pattern provided by the ferritoscope manufacturers, the ferrite values measured showed significant deviations from the real values. The current work presents a solution for using the ferritoscope for a more accurate quantification of the ferrite content in superduplex stainless steels.

1. Introduction

The evaluation of ferrite content in superduplex stainless steel is an important step in the manufacturing process of many industrial equipment. An accurate evaluation contributes for the project life-span prediction, avoiding premature failures or unscheduled stops. International standards establish limits for ferrite content in stainless steel, for instance, NORSOK M-630 [1] defines between 35 and 55% of the acceptable ferrite content for the base metal of duplex and superduplex stainless steel, and a range of 35–65% for the welded parts.

☆ Paper was part of technical contributions presented in the events part of the ABM Week 2017, October 2nd to 6th, 2017, São Paulo, SP, Brazil.

* *Corresponding author.*
E-mail: cgcamerini@metalmat.ufrj.br (C.G. Camerini).

https://doi.org/10.1016/j.jmrt.2018.06.005

In the case of austenitic stainless steels, a value from 2 to 5% of ferrite content in the weld bead is not only acceptable, but also expected [2], ensuring a higher resistance to stress corrosion cracks and reducing the risk of solidification cracking [2,3]. Different techniques of microstructural characterization are commonly applied to evaluate the ferrite content in stainless steel, such as optical microscopy, scanning electron microscopy, X-ray diffraction, metallographic replication, vibrating sample magnetometer, and the ferritoscope [4–7]. Among the listed techniques, it is reasonable to emphasize the ferritoscope as the most appropriate technique for the ferrite content evaluation in industrial environment, because besides its portability, the equipment is simple to operate and provides a direct non-destructive response for different types of stainless steels [8]. To use the ferritoscope, it is mandatory to calibrate the equipment with calibration pattern defined by the standard AWS A 4.2 [9]. The known ferrite amount in the calibration samples is correlated with ferritoscope magnetic response, and a specific calibration curve is configured in the equipment. Considering the guide presented by [10], it is introduced a procedure and a set of calibration samples to experimentally measure the ferrite content in austenitic and duplex and superduplex stainless steel. However, the experimental results achieved by the present study following the suggested calibration procedures did not achieve significant results inspecting superduplex stainless steel. In addition, it is highlighted through [9] that materials with the same volumetric fraction of ferrite can present different magnetic behaviors, depending on the grain size and manufacturing process. The current work made a careful analysis of the ferrite content results achieved by the ferritoscope and presents a specific solution for using the equipment for a more accurate quantification of ferrite in superduplex stainless steels.

2. Methods

Twenty-three samples of superduplex stainless steel class UNS S32750 with chemical composition presented in Table 1 were prepared. Different heat treatments were performed in the samples with the aim to produce different amounts of ferrite. The samples have 90 × 45 × 5.5 mm, and the ferrite volumetric fraction was quantified by X-ray diffraction (XRD).

XRD was performed in a D8 Discover (Bruker AXS) using cobalt radiation ($\lambda = 1.789$ Å), equipped with a Lynx Eye PS Detector. The equipment operated at constant values of tension (35 kV) and current (40 mA), respectively. The voltage and current values were 35 kV and 40 mA, respectively. The scanning data was obtained in the 2θ range of 45–105°, with a step size of 0.001° and scanning velocity of 0.5 s/step. Ferrite volumetric fraction was obtained by the Rietveld method [11], using the Diffrac Plus TOPAS® software. The ferrite volumetric fractions were measured in nine different areas of each sample and the ferrite average value was calculated as presented in Table 2. The XRD technique has been widely used for quantitative analysis of different phases in multiple-phase materials [12], and therefore, it is the choice for such task in this work. The ferrite average values achieved by XRD in the superduplex samples were defined as reference values to compare with the ferritoscope measurements. Fig. 1 shows an XRD spectrum of the phases presented in sample 16 that had an average volumetric fraction of ferrite (δ) and austenite (γ) around 49.7 and 50.3%, respectively.

Table 2 – Twenty-three superduplex reference samples were prepared with different heat treatments to achieve several amounts of ferrite. The ferrite contents were evaluated by XRD.

Sample	Ferrite content (%)	Sample	Ferrite content (%)
01	32.5 ± 2.7	13	52.2 ± 2.0
02	47.5 ± 3.5	14	55.7 ± 4.9
03	34.8 ± 4.1	15	52.8 ± 1.6
04	45.1 ± 11.5	16	49.7 ± 7.7
05	31.7 ± 7.8	17	43.1 ± 5.1
06	29.6 ± 8.2	18	45.7 ± 5.7
07	36.6 ± 4.9	19	61.1 ± 2.9
08	33.4 ± 4.5	20	71.6 ± 5.0
09	41.2 ± 6.9	21	55.1 ± 3.0
10	40.4 ± 5.3	22	58.2 ± 6.9
11	39.0 ± 7.1	23	65.7 ± 6.3
12	29.9 ± 3.6		

Analyses by optical microscopy were also made in some samples to corroborate the XRD results. The samples were grinded, polished, and electrolytic etched with 20% NaOH solution, applying 3 V for 15 s to reveal the microstructure. Fig. 2 shows the metallographic image of the samples 16 and 20, with 49.7 and 71.6% of ferrite, respectively.

The magnetic induction ferrite meter used in the work was the FERITSCOPE® FMP30 from Helmut Fischer® with the calibration pattern WRC 0.3/80, which contain samples with 0.52, 3.05, 10.2, 30.4, and 55.1% of ferrite and one sample, named as ferrite base, containing 100% of ferrite. It is important to mention that the ferritoscope test is mandatory to calibrate the equipment with the calibration pattern [10]. Moreover, to study the calibration pattern samples, the following equipment were used: X-ray fluorescence spectrometry for chemical composition analysis with Bruker's TRACER III-SD; vibrating sample magnetometer (VSM) from Lake Shore to analyze the material magnetization curve; and Elcometer® 456 to evaluate the presence of metallic coatings.

3. Results and discussions

The first approach was to calibrate the ferritoscope with the calibration samples provided by the manufacturer and test the

Table 1 – Chemical composition of superduplex stainless steel S32750.

Element	C	Mn	Si	Cr	Ni	Mo	N
UNS S32750 (wt%.)	0.022 ± 0.003	0.79 ± 0.01	0.25 ± 0.01	24.80 ± 0.2	7.2 ± 0.2	3.85 ± 0.04	0.32 ± 0.005

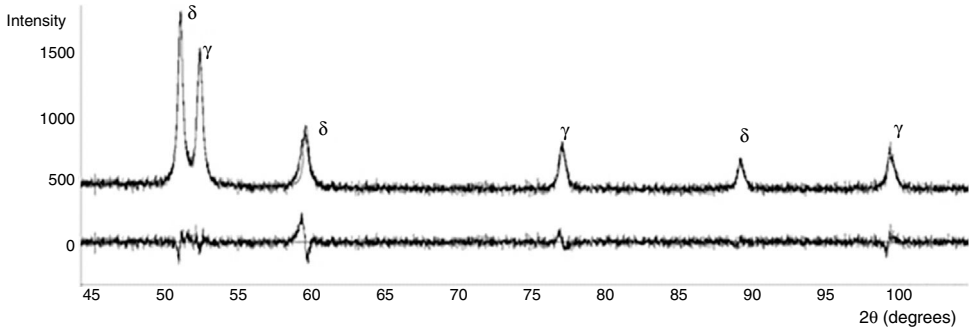

Figure 1 – XRD spectrum of sample 16 with 49.7% of ferrite.

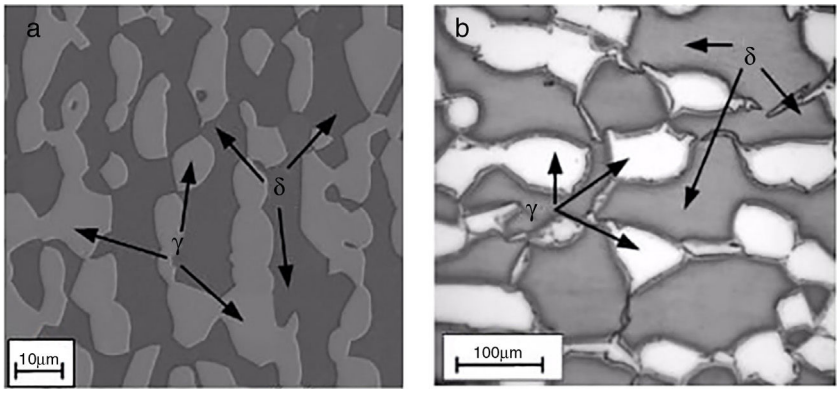

Figure 2 – (a) Sample 16 with $\delta/\gamma \approx 50/50$; (b) sample 20 with $\delta/\gamma \approx 70/30$.

equipment efficiency measuring the ferrite content in all 23 superduplex samples prepared. The ferrite values indicated by the ferritoscope were correlated with the ferrite measured by XRD. Fig. 3 shows the ferritoscope ferrite content as a function of the values measured by the XRD. The line on the graph indicates the theoretical agreement between the techniques. As noticed in the graph, the ferrite values are underestimated by the ferritoscope. However, it can be highlighted that the samples with low amount of ferrite presented a better correlation with the XRD measurements and as the ferrite content increases the correlation is impaired.

The results shown in Fig. 3 raise the hypothesis that the calibration curve set on the ferritoscope might have a good fit just for low ferrite content. In order to investigate the results, a detailed analysis of the standards samples used in the ferritoscope calibration process was performed. Through the X-ray fluorescence technique, it was estimated the chemical composition of calibration samples, where chromium (Cr), nickel (Ni), molybdenum (Mo), and iron (Fe) contents are shown in Table 3.

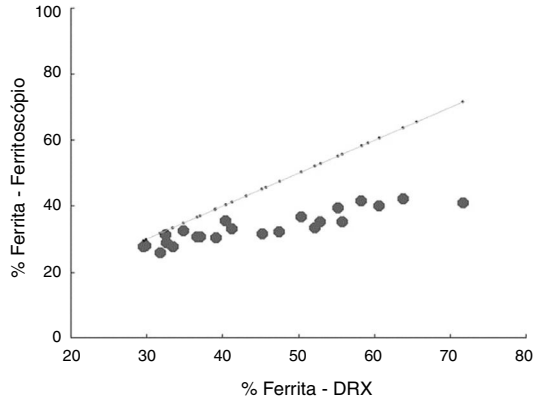

Figure 3 – Ferrite content measured by the ferritoscope as a function of the reference ferrite content evaluated by XRD.

Among the specimens used in the ferritoscope calibration, it is possible to emphasize three samples that showed unexpected characteristics on the first investigation. On the chemical composition results, the standard sample with 55.10% of ferrite presented a Cr content of 96.76%, and, due to this high amount, it was suspected that the sample presented a metallic Cr coating. An evaluation of the metallic coating was performed using the equipment Elcometer 456, which revealed a Cr coating of 25.5 μm of thickness. A mechanical grinding removed the coating, and a new chemical composition analysis was made, revealing a carbon steel with

Table 3 – Chemical composition of the standard samples used in the ferritoscope calibration.

% ferrite	Cr	Ni	Mo	Fe
0.52	19.5	10.3	0.03	68.1
3.05	20.9	10.9	0.1	65.3
9.20	22.6	11.7	0.1	62.2
30.40	21.7	5.5	2.9	68.0
55.10	96.7	0.02	–	2.4
100	–	38.5	–	61.0

0.095% Cr, 0.007% Ni, 0.39 Mo, and 96.96% Fe. The ferrite base specimen, who corresponds to 100% of ferrite, also presented an anticorrosive metallic coating. The third specimen that presented an unexpected result was the one with 30.40% of ferrite, because considering its chemical composition (Table 3), it corresponds to a duplex stainless steel, which, as annealed, presents a balanced microstructure with the ratio of ferrite/austenite around 50/50% [13,14]. However, according to the calibration pattern, the amount of ferrite in the sample is 30.40%. The first investigation to confirm the microstructure presented in the 30.40% calibration specimen was the optical microscopy. In this analysis, the specimen was mechanically grinded and polished, followed by electrolytic etching. Fig. 4 shows the duplex steel 2205 microstructure of the specimen used in the ferritoscope calibration pattern, which the phase counting was performed according to the standard ASTM E562 [15]. The sample presents 51.4% of ferrite, differing from the 30.40% described in the calibration standard.

Besides the metallographic analysis, aiming to confirm the ferrite content in the sample, a magnetization curve of the sample was performed, which, according to Abreu et al. [16] and Silva et al. [17], from the magnetic saturation level is possible to establish the content of the ferromagnetic phases presented in the material. A vibrating sample magnetometer was used to trace the magnetization curve of the calibration sample that indicates 30.40% of ferrite and the curve of the as annealed sample, number 16 (Table 2) with 49.7% of ferrite. These curves were compared in order to verify the similarities of the saturation levels. As presented by Fig. 5, the saturation level of the samples is close, indicating a similar ferrite amount. It is worth mention that the difference at the beginning of the magnetization curves is caused by the different geometries of the samples and to avoid such variation is necessary to apply different magnetization factors in the samples which were not considered in the curves. However, to evaluate the ferromagnetic content, the saturation level is sufficient, and it does not depend on the samples geometry [18], thus validating the similar ferrite content in the samples.

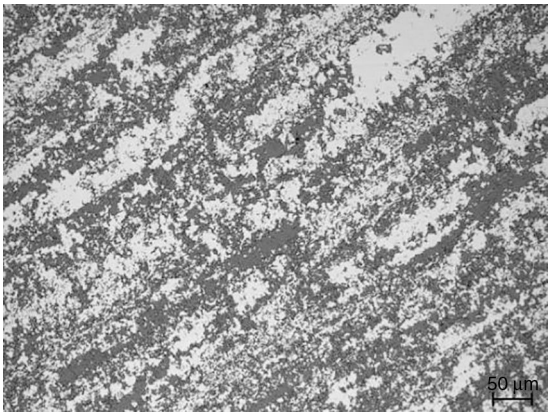

Figure 4 – Microstructure of the ferritoscope calibration sample. The calibration pattern define the ferrite content in the sample as 30.40%, which diverge from 51.4% of ferrite achieved by metallographic quantification with optical microscopy.

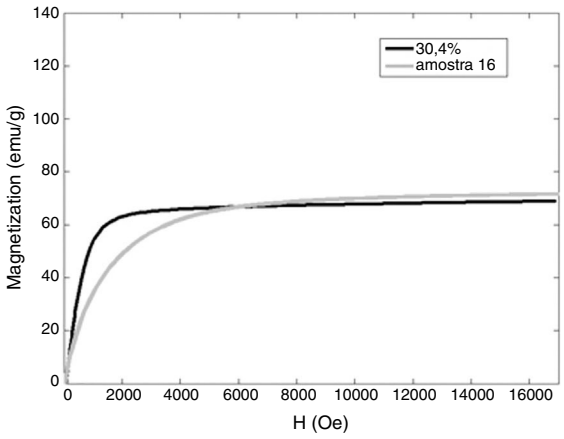

Figure 5 – Magnetization curves. In gray, the curve of the sample 16, as-annealed, and in black the magnetization curve of the calibration sample with 30.40% of ferrite used for the ferritoscope calibration.

Based on the chemical composition analysis, optical microscopy, and the magnetic saturation level, it is possible to conclude that the calibration sample that indicates 30.40% of ferrite actually has a volumetric fraction of ferrite close to the as-annealed situation, with approximately 50% of ferrite. This difference in the quantification might be one of the reasons for the underestimated result achieved by the ferritoscope showed in Fig. 3. The ferrite content evaluation is a polemic subject, widely discussed and detailed by [9]. In order to improve the results of the ferritoscope quantification, three samples of the 23 prepared in this work, were selected to replace some samples of the ferritoscope calibration pattern. Table 4 shows the ferrite content and the chemical composition of the samples selected for the new calibration of the ferritoscope, samples number 12, 16, and 20 (Table 2) replaced the standard calibration samples with high ferrite. These samples were applied to calibrate the ferritoscope and later all the superduplex samples were again tested. It is important to note that the sample with 29.9% of ferrite also presents intermetallic phases, such as sigma, in the microstructure. The superduplex phase stability diagram and the influence of the sigma phase in the superduplex magnetic behavior are well reported in the work published by Bettini et al. [19] and Rebello et al. [20].

Fig. 6 shows the ferrite content measured by the ferritoscope as a function of the ferrite reference values achieved by XRD. Comparing Figs. 3 and 6, it is possible to notice that the ferritoscope calibration with the superduplex samples improved the ferrite quantification. The results

Table 4 – Samples manufactured at the present work which replaced the originals samples in the ferritoscope calibration pattern.

% ferrite	Cr	Ni	Mo	Fe
29.90	24.8	7.2	3.8	65.7
49.7	24.8	7.2	3.8	65.7
71.6	24.8	7.2	3.8	65.7

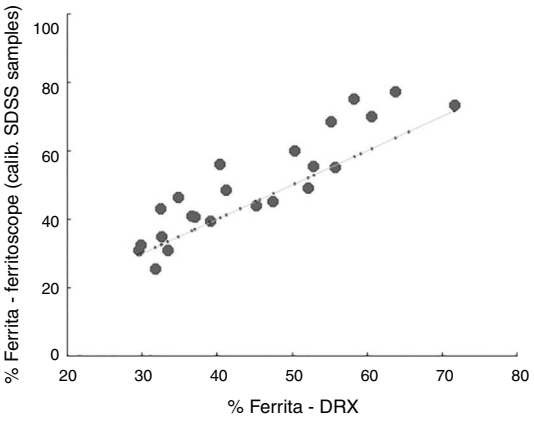

Figure 6 – Ferrite content measured by the ferritoscope as a function of the reference ferrite content evaluated by XRD. The ferritoscope calibrated with superduplex samples.

confirm the relevance of using a calibration standard sample with the same material as the one intended to inspect. Consequently, to achieve accurate ferrite quantification in superduplex steels, it is necessary to calibrate the equipment with samples of the same material under inspection, which differs from what is stated by [10].

4. Conclusion

According to the results, for stainless steels with low ferrite content, until 35% of ferrite, it is possible to use the calibration pattern provided by the ferritoscope manufactures. The fact that the ferritoscope calibration pattern is composed of different alloys lead to an underestimation of the ferrite content in dual phases material, such as superduplex. Results showed that for ferrite quantification in superduplex stainless steels, it is necessary to use a specific standard with the same material and same manufacture process for the ferritoscope calibration.

5. Conflicts of interest

The authors declare no conflicts of interest.

Acknowledgements

The authors would like to thank the Brazilian research agencies CAPES and CNPQ for the financial support.

REFERENCES

[1] Norsok Standard M-630: Material data sheets and element data sheets for piping. Standards Normay, 2010.
[2] The Welding Institute [página da internet]. Cambridge: TWI, 2017 [accessed 18 jun. 2017]. Available in: http://www.twi-global.com/technical-knowledge/job-knowledge/.
[3] Pessanha EC. Quantificação da ferrita delta e avaliação da relação microestrutura/propriedades de um aço inoxidável austenítico 347 soldado [dissertação de mestrado]. Campos dos Goytacazes: Universidade Estadual do Norte Fluminense; 2011.
[4] Forgas Junior A, Otubo J, Magnabosco R. Ferrite quantification methodologies for duplex stainless steel. J. Aerosp. Technol. Manage 2016;8(3):357–62 [accessed 11 jun. 2017]; Available in: http://www.scielo.br/scielo.php?script=sci_arttext&pid=S2175-91462016000300357&lng=en&nrm=iso.
[5] Tavares SSM, Pardal JM, Abreu HFG, Nunes CS, Silva MR. Tensile properties of duplex UNS s32205 and lean duplex UNS S32304 steels and the influence of short duration 475 °C aging. Mater. Res 2012;15(6):859–64.
[6] Pardal JM. Efeitos dos tratamentos térmicos nas propriedades mecânicas, magnéticas e na resistência à corrosão de aços inoxidáveis superduplex [tese de doutorado]. Niterói: Universidade Federal Fluminense; 2009.
[7] Stainless steel guide. Stainless steels properties—how to weld them where to use them. Lincoln Eletric Company®, USA. Welding Guide, 2003.
[8] Saluja R, Moeed KM. Formation, quantification and significance of delta ferrite for 300 series stainless steel weldments. Int. J. Eng. Technol. Manage. Appl. Sci 2015;3:23–36.
[9] AWS A4.2M-06: Standard Procedures for Calibrating Magnetic Instruments to Measure the Delta Ferrite Content of Austenitic and Duplex Ferritic–Austenitic Stainless Steel Weld Metal. American Welding Society, 2006.
[10] Helmut Fischer®. Measurement of the Ferrite Content in Austenitic and Duplex Steel. Helmut Fischer, Germany. Catálogo do Feritscope® FMP30, 2012.
[11] Rietveld HM. A profile refinement method for nuclear and magnetic structures. J. Appl. Crystallogr 1969;2(2):65–71.
[12] Connolly JR. Introduction to quantitative X-ray diffraction methods, EPS400, Introduction to X-Ray powder diffraction. Spring, 2012.
[13] Martins M, Casteletti LC. Microstructural characterization and corrosion behavior of a super duplex stainless steel casting. Mater. Charact 2009;60:150–5.
[14] Badjia R, Bouabdallah M, Bacroix B, Kahloun C, Bettahar K, Kherrouba N. Effect of solution treatment temperature on the precipitation kinetic of r-phase in 2205 duplex stainless steel welds. Mater. Sci. Eng. A 2008;496(1–2):447–54.
[15] ASTM E562-05: Standard Test Method for Determining Volume Fraction by Systematic Manual Point Count. ASTM International, 2005.
[16] Abreu HFG, de Carvalho SS, Neto PL, dos Santos RP, Freire VN, Silva PMO, et al. Deformation induced martensite in an AISI 301LN stainless steel: characterization and influence on pitting corrosion resistance. Mater. Res 2007;10(4):359–66.
[17] Silva VMA. Caracterização por correntes parasitas de aços inoxidáveis austeníticos deformados a frio [dissertação de mestrado]. Rio de Janeiro: Universidade Federal do Rio de Janeiro; 2016.
[18] Shah SAH. Vibrating sample magnetometery: analysis and construction [página da internet]. Syed Babar Ali School of Science and Engineering. Paquistão 2013 [accessed 15 jun. 2017]. Available in: http://physlab.org/wp-content/uploads/2016/03/Sproj_alamdar1.pdf.
[19] Bettini E, Kivisäkk U, Leygraf C, Pan J. Study of corrosion behavior of a 22% Cr duplex stainless steel: influence of nano-sized chromium nitrides and exposure temperature. Electrochim. Acta 2013;113:280–9.
[20] J.M.A. Rebello, C.G. Camerini, M.C.L. Areiza, R.W. Santos and R.O. Carneval, Saturated low frequency eddy current technique applied to phases characterization in duplex stainless steel, in: Quantitave Non Destructive Evaluation, 2012.